

# Evolutionary Dynamics of Higher-Order Interactions

Unai Alvarez-Rodriguez,<sup>1,2,\*</sup> Federico Battiston,<sup>3</sup> Guilherme Ferraz de Arruda,<sup>4</sup> Yamir Moreno,<sup>5,6,4</sup> Matjaž Perc,<sup>7,8</sup> and Vito Latora<sup>2,9,10</sup>

<sup>1</sup>*Basque Centre for Climate Change (BC3), 48940, Leioa, Spain*

<sup>2</sup>*School of Mathematical Sciences, Queen Mary University of London, London E1 4NS, UK*

<sup>3</sup>*Department of Network and Data Science,*

*Central European University, 1051 Budapest, Hungary*

<sup>4</sup>*ISI Foundation, Turin, Italy*

<sup>5</sup>*Institute for Biocomputation and Physics of Complex Systems,*

*University of Zaragoza, Zaragoza 50008, Spain*

<sup>6</sup>*Department of Theoretical Physics, University of Zaragoza, Zaragoza 50009, Spain*

<sup>7</sup>*Faculty of Natural Sciences and Mathematics,*

*University of Maribor, Koroška cesta 160, 2000 Maribor, Slovenia*

<sup>8</sup>*Department of Medical Research, China Medical University Hospital,*

*China Medical University, Taichung, Taiwan*

<sup>9</sup>*Dipartimento di Fisica ed Astronomia,*

*Università di Catania and INFN, 95123 Catania, Italy*

<sup>10</sup>*The Alan Turing Institute, The British Library, London, NW1 2DB, UK*

## Abstract

We live and cooperate in networks. However, links in networks only allow for pairwise interactions, thus making the framework suitable for dyadic games, but not for games that are played in groups of more than two players. To remedy this, we introduce higher-order interactions, where a link can connect more than two individuals, and study their evolutionary dynamics. We first consider a public goods game on a uniform hypergraph, showing that it corresponds to the replicator dynamics in the well-mixed limit, and providing an exact theoretical foundation to study cooperation in networked groups. We also extend the analysis to heterogeneous hypergraphs that describe interactions of groups of different sizes and characterize the evolution of cooperation in such cases. Finally, we apply our new formulation to study the nature of group dynamics in real systems, showing how to extract the actual dependence of the synergy factor on the size of a group from real-world collaboration data in science and technology. Our work is a first step towards the implementation of new actions to boost cooperation in social groups.

---

\*Electronic address: unaialvarezr@gmail.com

Cooperation in large groups of unrelated individuals distinguishes humans most from other mammals, and it is one of the central pillars of our evolutionary success [1]. The impetus for this remarkable other-regarding abilities can be attributed to the difficulties in rearing offspring that survived, which the genus *Homo* experienced from the onset of its existence [2]. Nature's pressure towards alloparenting care is thus one of the earliest, if not the earliest, example of human cooperation. And since such cooperation obviously requires communication and agreements, an argument can also be made that it is precisely because of it that we have evolved to the highest levels of intelligence in the animal world. In fact, an artificial neural network model was recently proposed showing that selection for efficient decision-making in cooperative dilemmas can give rise to selection pressures for greater cognitive abilities, and that intelligent strategies can themselves select for greater intelligence, thus providing mechanistic support for the social intelligence hypothesis [3]. Nonetheless, cooperation remains at odds with the fundamental principles of Darwinian evolution, and it is fascinating that, as a species, we have succeeded in collectively holding off self-interest over most of the last two million years.

Given this puzzle, the search for reasons and mechanisms that may allow cooperation to evolve and proliferate is an evergreen and vibrant subject across the social and natural sciences [4–9]. Evolutionary game theory is long established as the theory of choice for addressing the puzzle mathematically [10–12], wherein social dilemmas constitute a particularly important class of games. Namely, social dilemmas capture the essence of the problem since defection is the individually optimal strategy, whilst cooperation is the optimal strategy for the highest social welfare [13]. An important mechanism for cooperation in social dilemmas is network reciprocity [14], which stands for the fact that a limited interaction range, as dictated by lattices or other types of networks, facilitates the formation of compact clusters of cooperators that are in this way protected against invading defectors. This basic mechanism could also be seen if the degree distribution of the interaction network is strongly heterogenous [15–17], if there is set or community structure [18, 19], or if the evolution unfolds on two or more network layers that mutually support cooperative clusters [20–27].

Despite the wealth of important insights concerning the evolution of cooperation on networks and fundamental discoveries [28–30], an important unsolved problem remains accounting for cooperation in groups, such as for example in the public goods game (PGG) [31, 32]. The simplest remedy is to consider members of a group to be all the players that are pairwise-connected to a central player [33, 34]. However, since the other players are further connected in a pairwise

manner, one would also need to consider all the groups in which the central player is member but is not central. Evidently, classical networks do not provide a unique procedure for defining a group. Moreover, members of the same group are commonly not all directly connected with one another, which prevents strategy changes among them, either in terms of imitation, replication, or exploration. These facts posit a lack of common theoretical foundation for studying the evolution of cooperation in networked groups. Without knowing who is connected to whom in a group, it is also impossible to implement fundamental mechanisms that promote cooperation, such as reciprocity [35, 36], image scoring [37–39], and reputation [40–42].

As a solution, we here introduce and study higher-order interactions in evolutionary games that are played in groups. The distinctive feature of higher-order interactions is that, unlike in classical networks [43], a link can connect more than just two individuals [44]. Thus, higher-order networks naturally account for structured group interactions, wherein a group is simply made up of all players that are connected by a so called hyperlink, which is the higher-order analogous of the link. As a paradigmatic example, we consider a standard public goods game on the higher-order analogous of a network, referred to as a hypergraph, see Figure 1. We first show that it corresponds exactly to the replicator dynamics in the well-mixed limit. As such, it thus provides an exact theoretical foundation to study cooperation in networked groups – effectively a null model – that is amenable to further upgrades. Next, we consider the public goods game on heterogenous hypergraphs, which allow us to consider scenarios in which the synergy factor depends on the group size in a systematic and consistent manner. We show, for example, how synergy factors that are given by different powers of the group size lead to a critical scaling in the transition from defection to cooperation. Lastly, we also demonstrate how the proposed higher-order interaction framework can be used to determine the synergy factor as a function of the group size from empirical data on cooperation and collaborations. Under the assumption that the structure of the hypergraph is the outcome of an optimization process of the game it hosts, we extract the game parameters from datasets describing collaborations in science and technology, showing that higher-order interactions induce diverse benefits and costs in different social domains.

### **Evolutionary dynamics of higher-order interactions**

The public goods game describes a setting where  $N$  players are requested to contribute to a common pool with a token of value  $c$  [9]. Cooperators do contribute, and defectors do not. The

collected amount is then multiplied by the so called synergy factor  $R$ , and the benefit is shared amongst all the members of the group. The payoff for the defectors and cooperators playing in a group of  $g$  members is given by  $\pi_D = Rcw_C/g$  and  $\pi_C = Rcw_C/g - c$  respectively, with  $w_C$  representing the number of cooperators in the group. Typically  $c$  has a fixed value of  $c = 1$ , so that the behavior of the system is determined by the synergy factor  $R$ , or the reduced synergy factor  $r = R/g$ . Besides, it is common to represent the state of the system by the fraction of players adopting each strategy,  $x_C$  for the cooperators and  $x_D$  for the defectors.

The evolutionary dynamics determines how the strategies of the players evolve with each iteration of the PGG, that is, how the fractions  $x_C$  and  $x_D$  change with time. Here, we implement the so-called *fixed cost per game* approach, where cooperators contribute with an entire token to each game they play. Individual updates constitute micro-steps of the dynamics, whereas a (global) time step corresponds to  $N$  individual steps, so that all the players in the system have the chance to play the game and update their strategies. Players interact among them following the links of the network they are embedded in. As mentioned before, the standard network implementation [33], henceforth referred to as graph implementation (GI), is not able to account for the most general interaction in groups [45–47] (see the Supplemental Material for a detailed explanation).

In order to account for higher-order interactions, we use hypergraphs [44]. A hypergraph,  $H(\mathcal{N}, \mathcal{L})$ , is a mathematical object that consists of a set of  $N$  nodes  $\mathcal{N} = \{n_1 = 1, \dots, n_N = N\}$  and a set of  $L$  hyperlinks  $\mathcal{L} = \{l_1, \dots, l_L\}$ . Each hyperlink is a subset of two or more elements of  $\mathcal{N}$  and represents a group interaction. For instance, in Figure 1a, the hyperlink  $l_1$  contains nodes  $n_1$  and  $n_3$ , whereas the hyperlink  $l_3$  is the subset made up by nodes  $n_4, n_5$  and  $n_6$ . Furthermore, the cardinality of a subset, known as the order of the hyperlink, is the number  $g$  of nodes in the group. In the previous example,  $l_1$  has order 2 and  $l_3$  has order 3. In a hypergraph, the hyperdegree,  $k_i$ , of a node  $i$  represents the number of hyperlinks in which the node is involved into, thus, the number of groups of a specific order  $g$  that contains  $i$  can be denoted by  $k_i^g$ . Hence, the hyperdegree of  $i$  is given as  $k_i = \sum_{g=g^-}^{g^+} k_i^g$ , where  $g^-$  and  $g^+$  account for the minimal and maximal orders in  $\mathcal{L}$ . For example, in Figure 1a,  $k_4 = 3 = k_4^2 + k_4^3$ , with  $k_4^2 = 1$  (the hyperlink  $l_4$ ) and  $k_4^3 = 2$  (the hyperlinks  $l_2$  and  $l_3$ ).

Although hypergraphs are not the only possible representation of group interactions, they allow to exploit the analogy between the links representing pairwise interactions in contact networks and hyperlinks, which are based on higher-order, group interactions. As we will show next, the differences between these two approaches lead to fundamentally distinct outcomes of the PGG

evolutionary dynamics. To see how the evolutionary dynamics evolves in hypergraphs, let us consider the first step of a standard graph implementation of the PGG. When a node  $n_i$  and one of its neighbors  $n_j$  are selected on a graph, it is equivalent to say that a node and one of its links are selected. Such a procedure can be easily generalized to group interactions of more than  $g = 2$  individuals, see Figure 1b. Note that if we choose more neighbors of  $n_i$  to generate higher-order interactions, such an extension would still be based on dyadic ones. Instead, we propose a *hypergraph implementation (HI)* of the game that consists of selecting one of the hyperlinks of  $n_i$ . That is, in the HI setup, we select at random with uniform probability a node  $n_i$  in the hypergraph and one of its hyperlinks,  $l_i$ . Then, all the members of the hyperlink  $l_i$  play a game for each of the hyperlinks they are part of, as illustrated in Figure 1. Finally, as it is customary, the nodes accumulate the payoffs of all the rounds they play, and we normalize this quantity by the total number of played games, such that each node's performance is represented by its average payoff.

The second part of each micro-step of the evolutionary dynamics of the game involves updating the strategy of node  $n_i$ . To this end, we generalize the discrete replicator dynamics for the case of higher-order interactions. We propose to compare the payoff  $\pi_i$  of a node  $n_i$  with the maximal payoff of the selected hyperlink  $l_i$ . Under this rule,  $n_i$  will adopt the strategy of the node with the maximal payoff with probability  $\frac{1}{\Delta} \sum_{j \in l_i} (\pi_j - \pi_i) \prod_{k \in l_i} \theta(\pi_j - \pi_k)$ , where  $\Delta$  accounts for the maximal payoff difference. Note that the previous expression reduces to the standard one of the *GI* when  $g = 2$ .

## Results

To get some insights into the dynamics of the system in a simple configuration, we first studied the PGG on uniform random hypergraphs (URH) with hyperlinks of order equal to  $g = 2, 3, 4$  and  $5$  (see Methods for details on how to generate URH). Numerical simulations have been carried out for hypergraphs with  $N = 1000$  nodes (players), and the game has been iterated for  $T = 10^4$  time steps. The results obtained are reported in Fig. 2. Panel (a) shows the final fraction of cooperators as a function of the reduced synergy factor  $r$ . In each case, the simulations refer to hypergraphs with  $L = L_c$  hyperlinks, where  $L_c$  accounts for the minimal number of hyperlinks that guarantees the connectedness of the hypergraph. As it can be seen in the figure, there is a value of  $r$  beyond which cooperation emerges. We define this critical value of the reduced synergy factor,  $r_c$ , which depends on  $g$ , as the lowest value of  $r$  for which the fraction of cooperators is nonzero.

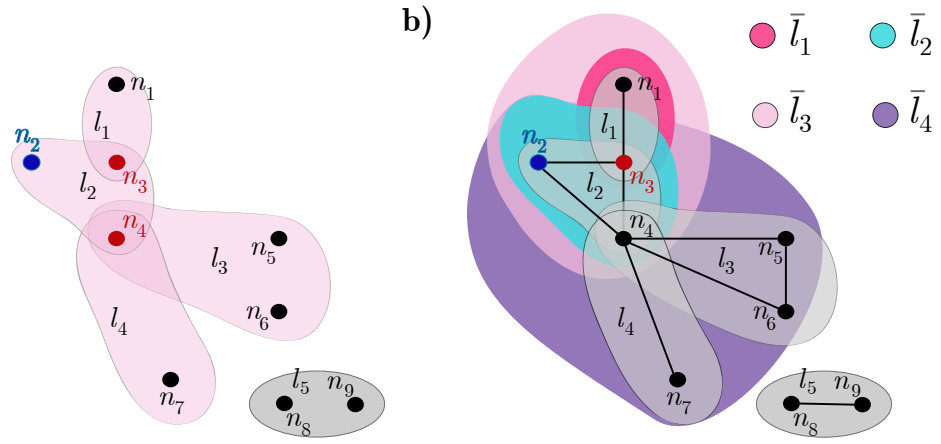


**FIG. 1: Higher-order vs pairwise interactions in a PGG.** Comparison of the proposed hypergraph implementation (HI) with a standard graph implementation (GI) of the game based on pairwise interactions only. **(a)** In the HI implementation, a node,  $n_2$ , and one of its hyperlinks,  $l_2$ , are randomly selected. All the nodes in the hyperlink  $l_2$ , namely node  $n_2$ , and the two nodes highlighted in red  $n_3$  and  $n_4$ , play all the games they are involved into, corresponding, in this example, to PGG defined for the subset of nodes of the hyperlinks  $l_1$ ,  $l_2$ ,  $l_3$  and  $l_4$ . Then, the strategy of  $n_2$  is updated by comparing its payoff with that of the node with the highest accumulated payoff of the hyperlink  $l_2$ . This is not equivalent to play the PGG in the graph generated by projecting the interactions of the hypergraph, which is shown in panel **(b)**. In the standard GI implementation, a neighbor of  $n_2$ , let us say  $n_3$  –highlighted in red– is randomly selected. The two nodes  $n_2$  and  $n_3$  then play all the games of the groups they are part of, that is, of the groups made up by the subsets of nodes  $\{n_1, n_3\}$ ,  $\{n_2, n_3, n_4\}$ ,  $\{n_1, n_2, n_3, n_4\}$  and  $\{n_2, n_3, n_4, n_5, n_6, n_7\}$ . These subsets, colored as indicated in the figure, could be represented by a different set of hyperlinks  $\bar{l}_1$ ,  $\bar{l}_2$ ,  $\bar{l}_3$  and  $\bar{l}_4$ , respectively, which are different from the set of hyperlinks of the original hypergraph. Finally, the strategy of  $n_2$  is updated by comparing its accumulated payoff to that of node  $n_3$ .

The results show that  $r_c$  decreases when the order  $g$  of the hyperlinks of the hypergraph increases. This is equivalent to say that  $r_c$  decreases when the same number of  $N = 1000$  individuals play in larger groups. We believe that this observation is important, since determining how  $r$  varies with the size of the group, allows to get more realistic insights. Admittedly, the well-mixed limit of population-size groups is rarely applicable in reality, thus, the study of the impact of having large groups inside large populations, as allowed by our higher-order framework, is key. The

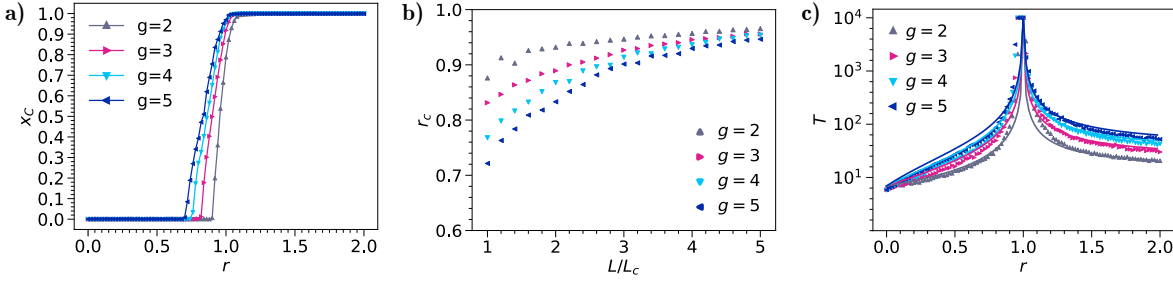


**FIG. 2: PGG with higher-order interactions in uniform random hypergraphs.** Numerical simulation of the HI of the game on uniform random hypergraphs of  $N = 1000$  players and different orders  $g$ . **(a)** Fraction of cooperators,  $x_C$ , as a function of the synergy factor,  $r$ , for hypergraphs with hyperdegree  $\langle k \rangle = k_c$ , or total number of links  $L = L_c$ , where  $k_c$  and  $L_c$  stand for the critical degree or number of links guaranteeing a connected hypergraph. **(b)** Critical value of the synergy factor,  $r_c$ , as a function of the ratio between the number of hyperlinks  $L$  and the critical value  $L_c$  in hypergraphs of different density. **(c)** Relaxation times as a function of the synergy factor,  $r$ , for hypergraphs with hyperdegree  $\langle k \rangle \geq 5k_c$ . In all plots, triangles correspond to numerical simulations, while the solid lines are the results of our theoretical predictions.

panel (b) of Fig. 2 displays how the value of  $r_c$  depends on the number of hyperlinks  $L$  in the hypergraphs. For each value of  $g$ , we observe an increase of  $r_c$  with  $L$ , and a tendency, for large hypergraph densities, to the value  $r_c = 1$ , which corresponds to the well-mixed replicator approximation [48]. Finally, the value of  $r$  also influences how long it takes for the system to converge to the stationary solution. This is illustrated in panel (c), where we show results of the relaxation time from an initial configuration with  $x_D = x_C = 0.5$ , in a hypergraph with  $L = 5L_c$ . These results are obtained by running the simulations up to a maximum of  $10^4$  steps. Furthermore, for the replicator approximation, the value of  $T$  can be analytically computed as  $T = \frac{\ln(N-1)}{|Q|}$ , with  $Q = (1-r)/\Delta$  (see the Supplemental Material for the details of the calculation). As it can be seen in the figure, the agreement between the theoretical predictions and the numerical results is qualitatively and quantitatively very good. This indicates that the dynamics of the PGG on uniform random hypergraphs corresponds to the replicator dynamics in the well-mixed limit.

The proposed HI of the PGG allows to study the more general, realistic and interesting case of hypergraphs where not all the hyperlinks have the same order. Important examples of such systems

include teams of different sizes working for a common goal or one-to-many communication via apps like WhatsApp, where users can create and belong to several groups of different sizes. In what follows, we consider heterogenous random hypergraphs with an assigned distribution of hyperlinks. Such hypergraphs are characterized by their total number of hyperlinks  $L$  and by a probability vector  $\mathbf{p} = \{p^g\}_{g=g-}^{g+}$ , whose entry  $p^g = k^g/k$  specifies how likely it is, on average, that the hyperdegree  $k$  of the node contains  $k^g$  groups of order  $g$ .  $\mathbf{p}$  is normalized such that  $\sum_{g=g-}^{g+} p^g = 1$ . Considering groups of different orders in the same hypergraph allows to focus on another important aspect of the PGG on higher-order structures, namely, the possible dependence of the rescaled synergy factor  $r$  on the order of the group. This is important for practical purposes, given the increasing interest in understanding how the size of a group impacts its performance. As it has been shown recently [49], large and small teams play different roles in science and technology ecosystems, thus, it is natural to assume that the synergy factor of a group depends on its size. This is particularly true in scientific publications, where it has been shown that the larger the group, the more citations a produced publication is likely to attract [50, 51]. Therefore, as a general form for such a dependence we assume that the synergy factor  $R$  is an increasing power law function of  $g$ , namely:

$$R(g) = \alpha g^\beta \quad (1)$$

with parameter  $\alpha > 0$  and exponent  $\beta \geq 0$ . The value of the exponent allows to tune the benefit that the players are able to produce when working as a group. In particular, adopting a superlinear scaling  $\beta > 1$ , means considering a synergistic effect of a group that goes beyond the sum of the individual contributions [52, 53]. Notice, however, that the assumed dependence in Eq. (1) is only a first approximation as it neglects saturation effects or even possible disadvantages due to difficulties in coordinating large groups, which, as we will see later on, appear in real systems. Under this assumption, the average payoff difference between cooperation and defection can be written as:

$$\pi_D - \pi_C = \sum_{g=g-}^{g+} p^g (1 - \alpha g^{\beta-1}) \quad (2)$$

where  $g_-$  and  $g_+$  are again the minimal and maximal orders of hyperlinks, respectively. The relaxation time is again given by  $T = \ln(N-1)/|Q|$ , where  $Q = (\pi_D - \pi_C)/\Delta$  (see the Supplemental Material for the definition of  $\Delta$  in the general case and for explicit calculations). It is then possible

to derive the critical value of the parameter  $\alpha$  as a function of the exponent  $\beta$  as:

$$\alpha_c(\beta) = \frac{1}{\sum_{g=g_-}^{g_+} p^g g^{\beta-1}} = \frac{1}{\mathcal{K}_\beta}, \quad (3)$$

where, for simplicity, we have defined  $\mathcal{K}_\beta \equiv \sum_{g=g_-}^{g_+} p^g g^{\beta-1}$ .

To explore how the dynamics evolves in heterogeneous random hypergraphs, we have performed numerical simulations of the PGG considering four different values of  $g = 2, 3, 4$  and  $5$  and allowing the values of  $p^g$  to take only multiples of  $1/4$ . This leads to  $35$  possible hypergraphs, one for each of all conceivable convex sums of  $\{p^2, p^3, p^4, p^5\}$  with the previous constraints. Results are reported in Fig. 3 for four different values of the power exponent  $\beta$ , namely,  $\beta = 0, 1, 2, 3$ , shown with different colors. Notice that the case  $\beta = 1$  corresponds to the underlying linear assumption of the standard PGG: in this case  $\alpha$  plays the role of the reduced synergy factor  $r$ . Panels a) through d) plot the color-coded fraction of cooperators as a function of the parameter  $\alpha$  in the definition of the synergy factor. The hypergraphs  $\mathcal{H}_i$  have  $\langle k \rangle = 2k_c$  and are displayed according to their value of  $\mathcal{K}_\beta$ , i.e., the value of the critical point  $\alpha_c(\beta)$ . As for the case of uniform random hypergraphs, we find that although the critical point is slightly over estimated for low densities by the analytical approximation, there is still a good agreement between the theoretical predictions of the well-mixed replicator approximation and the numerical simulations. We next explore the behavior of the relaxation time. Panels e) through h) shows results obtained for heterogeneous hypergraphs with  $\langle k \rangle = 5k_c$ . As it was done for the homogeneous scenario, we follow the dynamics of the system up to a maximum of  $T = 10^4$  time steps. The plots show that the relaxation times depend on  $\alpha$  for all values of  $\beta \neq 1$ , albeit rather differently with respect to the dependence of the critical value  $\alpha_c$  for  $\beta < 1$  and  $\beta > 1$ . In order to further explore this relationship, we analyzed how the average relaxation time varies as a function of the critical point  $\alpha_c$ . Results shown in panels i) to l) reveal that the dependence is always linear. However, when the synergy factor increases super linearly, there appear different curves, each one corresponding to a distinct family of hypergraphs and characterized by a different linear relation between the average relaxation time and the critical value. This behavior introduces an additional degree of freedom that can turn very useful, since the degeneracy that is observed for  $\beta \leq 1$  is broken for  $\beta > 1$ , and therefore one can independently set a critical point and a relaxation time by opportunely choosing the corresponding hypergraph.

From the previous results, a natural question arises: is it possible to determine the value of the synergy factor for a real PGG for each of the possible group sizes? A plausible answer to this

question can be obtained under the assumption that the very same structure of the hypergraph is the result of an evolutionary process in which nodes select the groups they belong to. We hypothesize that each individual tries to optimize the ideal number of groups of each order, based on the perceived dependence of the synergy factor on the group size. In this way, each real-world hypergraph would be the optimal structure that supports the game it hosts. We could then extract the functional form  $R(g)$  directly from the hyperdegree distribution of the hypergraph. More precisely, the goal would be to use the information in the vector  $\mathbf{p}$  of the hypergraphs on which the PGG occurs to determine the functional form,  $R(g)$ , of the synergy factor by imposing two conditions. The first condition comes from the assumption that the unknown reduced synergy factor  $r(g)$  is proportional to  $p_g$ . This originates in the intuition that the distribution of the hyperdegree of a generic player should be aligned with the potential benefit that each player expects to obtain for each higher-order interaction. The second condition imposes that the average payoff of cooperators is equal to the average payoff of defectors. This implies that the system is at equilibrium and guarantees the coexistence of cooperators and defectors. Thus, given that these two conditions are satisfied, it is possible to extract the curves of  $r(g)$  and  $R(g)$  from empirical data on higher-order interactions.

In order to show how the above mentioned procedure works in practice in real cases, we have studied collaboration in science and technology. In particular, we have considered a large data set of all the scientific articles published in the last century in thirteen journals of the American Physical Society (APS). For each journal, we have constructed a hypergraph whose nodes and hyperlinks represent respectively scientists and coauthored publications (see the Supplemental Material for further details). The reduced synergy factors have then been obtained from information on the number of authors in each publication (see Methods). From the plots of  $r(g)$  vs  $g$  reported in Fig.5a we notice the existence of a maximum value of  $r$  at intermediate group orders  $g$ . This indicates that there is an optimal tradeoff between the positive and negative effects of increasing the group size. The optimal value of  $g$  depends on the specific scientific community, as it varies from journal to journal. In the case of *PhysRevLett* the maximum of  $r(g)$  is located at  $g = 3$ . Different journals are associated to other optimal collaboration sizes. For instance, for *PhysRevApplied*  $r(g)$  is maximum at  $g = 5$ , indicating that larger collaborations are more beneficial in applied topics, such as device physics, electronics and industrial physics. For almost all journals, the synergy factor is low for  $g = 1$ , showcasing the difficulty of publishing alone in physics, a research area where team work has been becoming increasingly important in the last

decades [54]. Interestingly, a paradigmatic case is the one of *PhysRevSeriesI*, the very first journal published by the APS in the early 1900s, for which a sharp peak is located at  $g = 1$ , showing how most publications were produced by single scientists, in contrast with current trends. In order to shed light on this result we have factorized the synergy factor as the product of an increasing function of  $g$  times a decreasing function of  $g$ , and we have performed a numerical fit to extract the *benefit exponent*  $\beta$  and the so-called *cost parameter*  $\gamma$  (see Methods). This enables us to interpret the synergy factor as a combination of two contrary effects of the higher-order interactions in this particular dataset.

Fig.5b reports the values of  $\beta$  and  $\gamma$  obtained for each journal of the APS, and it allows to classify the different scientific communities in terms of benefits and costs of higher order interactions. These results provide a game-theoretic interpretation of the APS dataset. Specifically, in the context of this bibliographic dataset, hidden benefits and costs that conform the synergy factor can be associated to several aspects of the task of producing a publication. Benefits (increase of the synergy factor with increasing  $g$ ) would correspond to the potential reinforcement of the amount and quality of the ideas and the potential increase in the outreach of the work with the number of co-authors involved. On the contrary, the costs (decrease with increasing  $g$ ) would be the additional organizational effort in the process of arriving to a consensus and carrying out the tasks for publishing a paper. Experimental communities, such as that of nuclear physicists publishing in *PhysRevC*, tend to have low costs. These ideas are aligned with recent studies about the creation and production of research ideas [55] and the role, group dynamics and success of teams [49–51]. Our formalism allows for a quantitative analysis of these phenomena and could be used in future applications to design ways to foster higher-order cooperation.

## Discussion

Summing up, we have introduced higher-order interactions in evolutionary games to study cooperation in groups. Since higher-order interactions allow for a single link to connect more than just two individuals, they are naturally suitable to define groups in networks. In doing so, higher-order interactions thus do away with the arbitrary definitions of groups in classical networks, and they provide an exact theoretical foundation to study cooperation in networked groups. We have shown that the public goods game on a hypergraph is effectively a null model that agrees exactly with the replicator dynamics in the well-mixed limit. As such, it can be used in future research

towards upgrades that add additional layers of reality in models of human cooperation, either by means of strategic complexity [9], or by means of more complex interaction networks [56].

Towards the latter effect, we have also studied the public goods game on heterogeneous hypergraphs, where hyperlinks can have different lengths. Due to the exact definition of a group in the proposed framework, we have been able to systematically and consistently consider synergy factors that are dependent on group size. Indeed, the framework allows us to understand group size effects on cooperation in its most general form. As an example, we have considered synergy factors that are given by different powers of the group size, showing a critical scaling in the transition from defection to cooperation. In this case too, we have observed a significant agreement between the simulations and the analytical predictions of the model. Our framework enables novel analyses of real systems, as we have shown for the APS publications dataset, providing new insights regarding the positive and negative effects associated to higher-order interactions and the nature of group dynamics.

It is also worth mentioning that in his essay titled *Innate Social Aptitudes of Man*, W. D. Hamilton wrote, “There may be reasons to be glad that human life is a many-person game and not just a disjoined collection of two-person games”. He was referring to the fact that social enforcement works better in groups with more than two members, which can offer at least a partial cure for the problems with reciprocation in larger groups. Indeed, humans have a special gift for reciprocation, but even defining it in large groups is a non-trivial task [36]. If the group contains a cooperator and a defector, and in the absence of information who is who, whom do you reciprocate with? We note that the theoretical framework of higher-order interactions resolves this long-standing challenge in evolutionary game theory, and in the future invites reexamining fundamental mechanisms that may promote cooperation, such as image scoring [37–39], rewarding [57], and punishment [58–61].

Given the fundamental differences between pairwise and higher-order interactions, it would also be of interest to revisit the role of specific network properties and their role in the evolution of cooperation. In this regard, the role of strongly heterogenous degree distributions [15–17], community structure [19], as well as two or more network layers [20–27], promise to be fruitful ground for future explorations on how interaction structure impacts cooperation. Overall, we believe that the introduction of higher-order interactions to evolutionary games has a strong transformative potential for better understanding the evolution of cooperation and other social processes in networks, and we hope that our research will prove to be an important first step in this exciting and

promising direction.

## Methods

*Uniform random hypergraphs (URH):* As a prerequisite for working out the numerical simulations we explain here the procedure for creating hypergraphs where all the hyperlinks have the same order, which are known as uniform hypergraphs. An URH of order  $g$  is constructed by assigning a uniform probability  $p$  to each  $g$ -tuple of  $\mathcal{N}$ . For each of them, a random number in the  $[0, 1)$  interval is generated, and if this number is lower than  $p$ , the hyperlink containing the  $g$ -tuple is created. However, this method scales badly with  $g$  given the large amount of  $g$ -tuples to be considered. A more efficient variant is to have a predefined value of hyperlinks  $L$ , and generate a random integer in the  $[1, C_g^N]$  interval. One has to provide an ordering for the set of all possible hyperlinks, so that each of the random integers corresponds to a position in this ordering. The hyperlinks that are reached through this process are created. For the purpose of studying the stationary condition of a game, we are interested in having a connected hypergraph. The critical thresholds for hyperlinks  $L_c$  and hyperdegree  $k_c$  are given by  $L_c = N \ln N/g$  and  $k_c = \ln N$ . When  $p$  is tuned to exceed these numbers there is a high probability that the resultant hypergraph is connected.

*Extracting synergy factors from real data:* We show here how the dependence of the reduced synergy factor  $r(g)$  on group size  $g$  can be derived for real systems, based on the assumption that this information is encoded in the very same structure of a hypergraph. In particular, we have considered a data set of scientific publications and we have used it to investigate how benefits change with the size of groups in scientific collaborations. The data set consists of 577886 papers published in the period from 1904 to 2015 in the collection of all the journals of the American Physical Society (APS) [62]. We have constructed the 13 hypergraphs corresponding to different journals, such as Physical Review, Physical Review Letters, etc. of the APS. The nodes and hyperedges of these hypergraphs represent scientists and publications respectively. The order of a hyperedge is equal to the number of authors of the corresponding publication. For each hypergraph, we have extracted the number  $L^g$  of hyperedges of a given order  $g$ , that we used to compute the average number  $k^g = gL^g/N$  of hyperedges of order  $g$  a node is involved in. The reduced synergy factor  $r(g)$  can then be extracted from the proportion  $p^g = k^g/k$  of hyperedges

of order  $g$  of a node, by assuming that  $r(g) = cp^g$  and using the critical point relation:

$$\sum_{g=g^-}^{g=g^+} p^g (1 - r(g)) = 0 \quad (4)$$

to calculate the proportionality constant  $c$ .

*Cost-benefit factorization of the synergy factor:* In scientific collaborations across all journals of the APS, an optimal team size is associated to a maximum in the synergy factor, suggesting that an excessively large number of co-authors might lead to disadvantages in cooperation. In order to account for these effects, we have modelled the synergy factor extracted from real-world collaboration data as the following function of  $g$ :

$$f(g, \alpha, \beta, \gamma) = \alpha g^\beta e^{-\gamma(g-1)}. \quad (5)$$

ruled by the three parameters,  $\alpha, \beta$  and  $\gamma$ . The first parameter,  $\alpha$ , introduced in Eq. (1), is determined by the critical point condition. The remaining two parameters account respectively for the benefits and costs of the higher-order interactions. Benefits are modelled as a power-law of the group size  $g$  with an exponent  $\beta$ . Costs are described by an exponential decrease in the group size tuned by the cost parameter  $\gamma$ . To extract the pair of parameters  $(\beta, \gamma)$  for each journal, we have explored the parameter space and performed an optimisation in order to correctly reproduce the empirical points. For each considered pair  $(\beta, \gamma)$  we have computed the normalized distance between the synergy factor inferred analytically and the one associated to the data (see the Supplemental Material for further details on the procedure). The pairs with the smallest distance are selected as the outcome of the optimization process and are those reported in Fig.5c.

---

[1] Nowak, M. A. and Highfield, R. *SuperCooperators: Altruism, Evolution, and Why We Need Each Other to Succeed*. Free Press, New York, (2011).

[2] Hrdy, S. B. *Mothers and Others: The Evolutionary Origins of Mutual Understanding*. Harvard University Press, Cambridge, MA, (2011).

[3] McNally, L., Brown, S. P., and Jackson, A. L. Cooperation and the evolution of intelligence. *Proc. R. Soc. B* **279**, 3027–3034 (2012).

[4] Henrich, J., Boyd, R., Bowles, S., Camerer, C., Fehr, E., Gintis, H., and McElreath, R. In search of homo economicus: Behavioral experiments in 15 small-scale societies. *Am. Econ. Rev.* **91**, 73–78 (2001).

- [5] Nowak, M. A. Five rules for the evolution of cooperation. *Science* **314**, 1560–1563 (2006).
- [6] Henrich, N. and Henrich, J. P. *Why humans cooperate: A cultural and evolutionary explanation.* Oxford University Press, Oxford, U.K., (2007).
- [7] Rand, D. G. and Nowak, M. A. Human cooperation. *Trends in Cognitive Sciences* **17**, 413–425 (2013).
- [8] Kraft-Todd, G., Yoeli, E., Bhanot, S., and Rand, D. Promoting cooperation in the field. *Current Opinion in Behavioral Sciences* **3**, 96–101 (2015).
- [9] Perc, M., Jordan, J. J., Rand, D. G., Wang, Z., Boccaletti, S., and Szolnoki, A. Statistical physics of human cooperation. *Phys. Rep.* **687**, 1–51 (2017).
- [10] Weibull, J. W. *Evolutionary Game Theory.* MIT Press, Cambridge, MA, (1995).
- [11] Hofbauer, J. and Sigmund, K. *Evolutionary Games and Population Dynamics.* Cambridge University Press, Cambridge, U.K., (1998).
- [12] Nowak, M. A. *Evolutionary Dynamics.* Harvard University Press, Cambridge, MA, (2006).
- [13] Axelrod, R. *The Evolution of Cooperation.* Basic Books, New York, (1984).
- [14] Nowak, M. A. and May, R. M. Evolutionary games and spatial chaos. *Nature* **359**, 826–829 (1992).
- [15] Santos, F. C. and Pacheco, J. M. Scale-free networks provide a unifying framework for the emergence of cooperation. *Phys. Rev. Lett.* **95**, 098104 (2005).
- [16] Santos, F. C., Pacheco, J. M., and Lenaerts, T. Evolutionary dynamics of social dilemmas in structured heterogeneous populations. *Proc. Natl. Acad. Sci. USA* **103**, 3490–3494 (2006).
- [17] Gómez-Gardeñes, J., Campillo, M., Floría, L. M., and Moreno, Y. Dynamical organization of cooperation in complex networks. *Phys. Rev. Lett.* **98**, 108103 (2007).
- [18] Tarnita, C. E., Antal, T., Ohtsuki, H., and Nowak, M. A. Evolutionary dynamics in set structured populations. *Proc. Natl. Acad. Sci. USA* **106**, 8601–8604 (2009).
- [19] Fotouhi, B., Momeni, N., Allen, B., and Nowak, M. A. Evolution of cooperation on large networks with community structure. *J. R. Soc. Interface* **16**, 20180677 (2019).
- [20] Wang, Z., Szolnoki, A., and Perc, M. Evolution of public cooperation on interdependent networks: The impact of biased utility functions. *EPL* **97**, 48001 (2012).
- [21] Gómez-Gardeñes, J., Reinares, I., Arenas, A., and Floría, L. M. Evolution of cooperation in multiplex networks. *Sci. Rep.* **2**, 620 (2012).
- [22] Gómez-Gardeñes, J., Gracia-Lázaro, C., Floría, L. M., and Moreno, Y. Evolutionary dynamics on interdependent populations. *Phys. Rev. E* **86**, 056113 (2012).
- [23] Wang, Z., Szolnoki, A., and Perc, M. Interdependent network reciprocity in evolutionary games. *Sci.*

*Rep.* **3**, 1183 (2013).

- [24] Wang, Z., Wang, L., and Perc, M. Degree mixing in multilayer networks impedes the evolution of cooperation. *Phys. Rev. E* **89**, 052813 (2014).
- [25] Battiston, F., Perc, M., and Latora, V. Determinants of public cooperation in multiplex networks. *New J. Phys.* **19**, 073017 (2017).
- [26] Fu, F. and Chen, X. Leveraging statistical physics to improve understanding of cooperation in multiplex networks. *New J. Phys.* **19**, 071002 (2017).
- [27] Fotouhi, B., Momeni, N., Allen, B., and Nowak, M. A. Conjoining uncooperative societies facilitates evolution of cooperation. *Nat. Human Behav.* **2**, 492 (2018).
- [28] Lieberman, E., Hauert, C., and Nowak, M. A. Evolutionary dynamics on graphs. *Nature* **433**, 312–316 (2005).
- [29] Ohtsuki, H., Hauert, C., Lieberman, E., and Nowak, M. A. A simple rule for the evolution of cooperation on graphs and social networks. *Nature* **441**, 502–505 (2006).
- [30] Allen, B., Lippner, G., Chen, Y.-T., Fotouhi, B., Nowak, M. A., and Yau, S.-T. Evolutionary dynamics on any population structure. *Nature* **544**, 227–230 (2017).
- [31] Archetti, M. and Scheuring, I. Review: Game theory of public goods in one-shot social dilemmas without assortment. *J. Theor. Biol.* **299**, 9–20 (2012).
- [32] Perc, M., Gómez-Gardeñes, J., Szolnoki, A., and Floría and Y. Moreno, L. M. Evolutionary dynamics of group interactions on structured populations: a review. *J. R. Soc. Interface* **10**, 20120997 (2013).
- [33] Santos, F. C., Santos, M. D., and Pacheco, J. M. Social diversity promotes the emergence of cooperation in public goods games. *Nature* **454**, 213–216 (2008).
- [34] Szolnoki, A., Perc, M., and Szabó, G. Topology-independent impact of noise on cooperation in spatial public goods games. *Phys. Rev. E* **80**, 056109 (2009).
- [35] Trivers, R. L. The evolution of reciprocal altruism. *Q. Rev. Biol.* **46**, 35–57 (1971).
- [36] Sigmund, K. Punish or perish? retaliation and collaboration among humans. *Trends Ecol. Evol.* **22**, 593–600 (2007).
- [37] Nowak, M. A. and Sigmund, K. Evolution of indirect reciprocity by image scoring. *Nature* **393**, 573–577 (1998).
- [38] Milinski, M., Semmann, D., Bakker, T. C. M., and Krambeck, H.-J. Cooperation through indirect reciprocity: image scoring or standing strategy? *Proc. R. Soc. Lond. B* **268**, 2495–2501 (2001).
- [39] Nax, H. H., Perc, M., Szolnoki, A., and Helbing, D. Stability of cooperation under image scoring in

group interactions. *Sci. Rep.* **5**, 12145 (2015).

[40] Fehr, E. Don't lose your reputation. *Nature* **432**, 449–450 (2004).

[41] Gächter, S. Reputation and reciprocity: Consequences for the labour relation. *Scand. J. Econ.* **104**, 1–26 (2002).

[42] Fu, F., Hauert, C., Nowak, M. A., and Wang, L. Reputation-based partner choice promotes cooperation in social networks. *Phys. Rev. E* **78**, 026117 (2008).

[43] Latora, V., Nicosia, V., and Russo, G. *Complex networks: Principles, methods and applications*. Cambridge University Press, Cambridge, U.K., (2017).

[44] Berge, C. *Hypergraphs: Combinatorics of finite sets*. Elsevier, Amsterdam, (1984).

[45] Gómez-Gardeñes, J., Romance, M., Criado, R., Vilone, D., and Sánchez, A. Evolutionary games defined at the network mesoscale: The public goods game. *Chaos* **21**, 016113 (2011).

[46] Gómez-Gardeñes, J., Vilone, D., and Sánchez, A. Disentangling social and group heterogeneities: Public goods games on complex networks. *EPL* **95**, 68003 (2011).

[47] Peña, J. and Rochat, Y. Bipartite graphs as models of population structures in evolutionary multiplayer games. *PLoS ONE* **7**, e44514 (2012).

[48] Taylor, P. and Jonker, L. Evolutionary stable strategies and game dynamics. *Math. Biosci.* **40**, 145–156 (1978).

[49] Wu, L., Wang, D., and Evans, J. A. Large teams develop and small teams disrupt science and technology. *Nature* **566**(7744), 378–382 (2019).

[50] Wuchty, S., Jones, B. F., and Uzzi, B. The increasing dominance of teams in production of knowledge. *Science* **316**, 10361039 (2007).

[51] Klug, M. and Bagrow, J. P. Understanding the group dynamics and success of teams. *R. Soc. Open Sci.* **3**, 160007 (2016).

[52] Bettencourt, L. M. A., Lobo, J., Helbing, D., Kühnert, C., and West, G. B. Growth, innovation, scaling, and the pace of life in cities. *Proc. Natl. Acad. Sci. USA* **104**, 7301–7306 (2007).

[53] Bettencourt, L. M. A. The origins of scaling in cities. *Science* **340**, 1438 (2013).

[54] Battiston, F., Musciotto, F., Wang, D., Barabási, A.-L., Szell, M., and Sinatra, R. Taking census of physics. *Nat. Rev. Phys.* **1**, 89–97 (2019).

[55] Milojević, S. Principles of scientific research team formation and evolution. *Proc. Natl. Acad. Sci. USA* **111**, 3984–3989 (2014).

[56] Wang, Z., Wang, L., Szolnoki, A., and Perc, M. Evolutionary games on multilayer networks: a

colloquium. *Eur. Phys. J. B* **88**, 124 (2015).

[57] Rand, D. G., Dreber, A., Ellingsen, T., Fudenberg, D., and Nowak, M. A. Positive interactions promote public cooperation. *Science* **325**, 1272–1275 (2009).

[58] Andreoni, J., Harbaugh, W., and Vesterlund, L. The carrot or the stick: Rewards, punishments, and cooperation. *Am. Econ. Rev.* **93**, 893–902 (2003).

[59] Gächter, S., Renner, E., and Sefton, M. The long-run benefits of punishment. *Science* **322**, 1510 (2008).

[60] Boyd, R., Gintis, H., and Bowles, S. Coordinated punishment of defectors sustains cooperation and can proliferate when rare. *Science* **328**, 617–620 (2010).

[61] Jordan, J. J., Hoffman, M., Bloom, P., and Rand, D. G. Third-party punishment as a costly signal of trustworthiness. *Nature* **530**, 473–476 (2016).

[62] APS Dataset <https://journals.aps.org/datasets>.

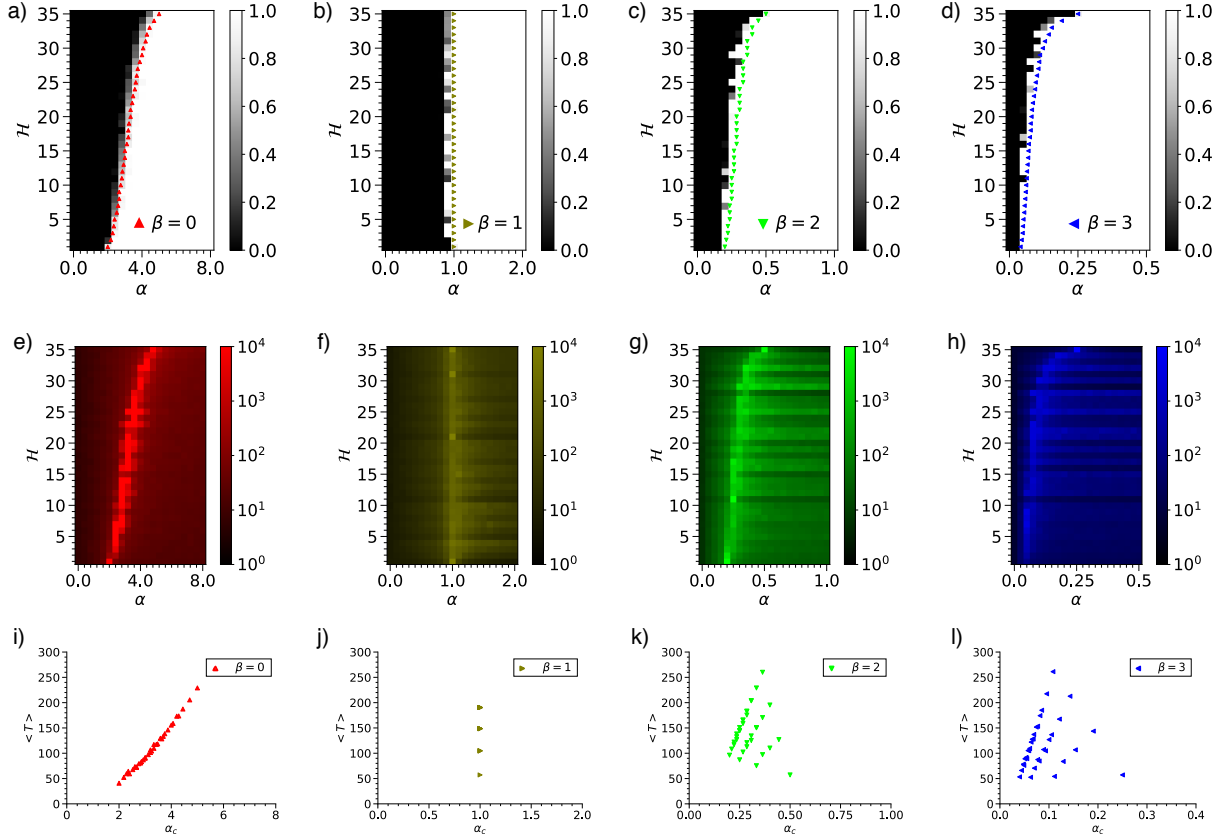


**FIG. 3: PGG with higher-order interactions in heterogeneous random hypergraphs.** We assume that the synergy factor grows according to Eq. (1) and consider the set of hypergraphs  $\mathcal{H}_i$  that contain hyperlinks of orders  $g = \{2, 3, 4, 5\}$  with probabilities  $p_g$  taking values in the set  $\{0, 1/4, 1/2, 3/4, 1\}$  —there are 35 possible such hypergraphs. **(a-d)** Fraction of cooperators as a function of  $\alpha$  for each of the 35 hypergraphs  $\mathcal{H}_i$  and several values of  $\beta$ . The hypergraphs are ordered according to their value of  $\mathcal{K}_\beta$ . Simulations have been carried out up to  $T = 10^4$  time steps for hypergraphs with  $\langle k \rangle = 2k_c$ , and triangles correspond to the theoretical predictions in the replicator approximation (see the Supplemental Material for details). **(e-h)** Relaxation time as a function of  $\alpha$  for the set of hypergraphs  $\mathcal{H}_i$ . Now hypergraphs have  $\langle k \rangle = 5k_c$ . **(i-l)** Predictions for the critical value  $\alpha_c$  as a function of the average relaxation time, calculated for each hypergraph in  $\mathcal{H}_i$  by averaging over the intervals of  $\alpha$  [0,8], [0,2], [0,1] and [0,0.5] for  $\beta = 0, 1, 2, 3$  respectively.

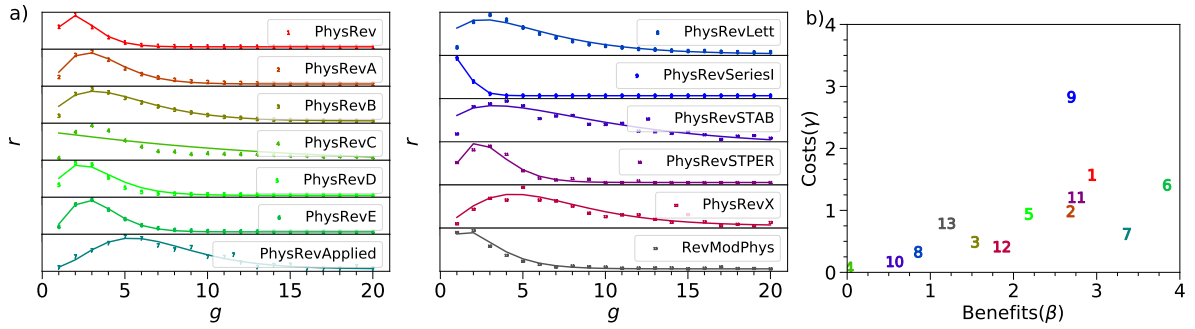


FIG. 4: **Synergy factors of scientific collaborations.** (a) Empirical synergy factors extracted from the structure of hypergraphs describing coauthorships from publications in the APS journals. Solid lines are fit of the empirical dots according to Eq. (5). Different symbols and colors refer to different journals, i.e. to different scientific communities. (b) Journal (labelled from 1 to 13) position in the costs-benefits diagram. The synergy factors are factorized as a function of two competing terms, one modelling the benefits of cooperation, which is dominant for small group size, and another one accounting for costs associated to an excessively large number of co-authors, which describes for the exponential decays observed in the first two panels.

## Appendix

### A. Graph Implementation

In the original network implementation, or GI, the core idea is to derive the higher order structure from the network of players. In the GI every node constructs its own focal hyperlink, whose constituents are the node itself and its first neighbours. Therefore, for a system of  $N$  players the GI imposes  $N$  different groups, each of them of  $g = k_i^2 + 1$  members. A micro-step in the game is played by following a sequence of steps: Firstly a node, and one of its neighbours, say  $n_i$  and  $n_j$ , are randomly selected from  $\mathcal{N}$ . Secondly the nodes play a round of the game for all the groups they belong to, accumulate their payoffs,  $\pi_i$  and  $\pi_j$ , and normalize them with the number of games they have played. As there is a group for each player every node will play  $k_i^2 + 1$  rounds. The third step is the update of the strategy, and for that purpose we employ the replicator update rule. According to this,  $n_i$  will adopt the strategy of  $n_j$  with probability  $\frac{1}{\Delta}(\pi_j - \pi_i)\theta(\pi_j - \pi_i)$ , where  $\Delta$  is the absolute value of the maximal payoff difference for all the possible strategies. It is noteworthy to mention that the replicator update rule is not the only update mechanism, but it is the one that we have selected because it provides an effective and noisy payoff oriented update rule by means of a simple analytic expression.

### B. Replicator Dynamics for URH

Let us introduce now the replicator model for predicting the dynamics of the system. This technique is based on the indistinguishability between different nodes, and therefore it should describe the system as long as the hypergraph is connected and the hyperlinks are uniformly distributed among the nodes. We are working with URH, and therefore the more connected the system is, the better it fulfils the uniform requirement, and the closer it gets to the replicator description.

In this simplified analysis we will describe the system in terms the fraction of defectors  $x_D$  and the fraction of cooperators  $x_C$ . We compute the average normalized payoff of defectors and cooperators  $\pi_D$  and  $\pi_C$ , as a function of their fractions,  $x_D$  and  $x_C$ , in an hyperlink of order  $g$ . In order to do so, we sum the payoff of all the possible configurations of  $g - 1$  nodes. The sum is taken over  $g - 1$  because one of the nodes is already occupied by a defector, in  $\pi_D$ , or a cooperator

in  $\pi_C$ . The payoff is calculated with the reduced synergy factor  $r$ .

$$\begin{aligned}\pi_D &= \sum_{i=0}^{g-1} \binom{g-1}{i} x_D^{g-1-i} x_C^i r \\ \pi_C &= \sum_{i=0}^{g-1} \binom{g-1}{i} x_D^{g-1-i} x_C^i ((i+1)r - 1)\end{aligned}\quad (6)$$

The total average payoffs, are obtained by multiplying the ones of Eq. (6) with the average degree. But, we also normalize the total payoff with the degree, so the terms that go into the dynamical equation are indeed  $\pi_D$  and  $\pi_C$ . One can observe that the  $\pi_D - \pi_C$  function is invariant with respect to the order  $g$ .

$$\begin{aligned}\pi_D - \pi_C &= \sum_{i=0}^{g-1} \binom{g-1}{i} x_D^{g-1-i} x_C^i [ir - ((i+1)r - 1)] = (1-r) \sum_{i=0}^{g-1} \binom{g-1}{i} x_D^{g-1-i} x_C^i \\ &= (1-r)(x_D + x_C)^{g-1} = 1 - r\end{aligned}\quad (7)$$

We now compute  $\Delta$ , the maximal payoff difference to be used in the replicators update rule. The  $\pi^+$  and  $\pi^-$  indicate the maximal and minimal payoff values from all the possible configuration of strategies.

$$\Delta \equiv \begin{cases} \pi_D^+ - \pi_C^- & \text{if } \pi_D^+ - \pi_C^- > \pi_C^+ - \pi_D^- \\ \pi_C^+ - \pi_D^- & \text{if } \pi_D^+ - \pi_C^- < \pi_C^+ - \pi_D^- \end{cases}\quad (8)$$

$\Delta$  is only expressed for comparisons of payoffs of different strategies, since the strategies are copied from the neighbours, and therefore the terms  $\pi_i^+ - \pi_i^-$ , where two nodes share the same strategy, are irrelevant. For any order  $g$ ,  $\Delta$  is given by

$$\Delta = \begin{cases} r(g-2) + 1 & \text{if } r < 1 \\ gr - 1 & \text{if } r > 1 \end{cases}\quad (9)$$

We now work with  $Q$ , the normalized payoff difference,  $Q \equiv (\pi_D - \pi_C)/\Delta$ .

The system equation is derived as the sum of all the channels via which the strategy of a node can change. These channels correspond to the different configurations of strategies of hyperlinks of order  $g$ , weighted with the probabilities of the nodes having a particular strategy. For each configuration, one has to compute the probability of having a defector-cooperator pair,  $w_D w_C / g(g-1)$  and the probability that this pair results in an strategy change. Notice that the values of  $w_D$  and  $w_C$ , the number of defectors and cooperators in the group, are precisely the exponents of  $x_C$  and  $x_D$ .

We employ the replicator update, which in this context means that the flip probability is computed as  $-Q\theta(\pi_C - \pi_D)$  when a defector changes into a cooperator and as  $Q\theta(\pi_D - \pi_C)$  in the opposite case. This sign corresponds to the calculation of the fraction of defectors, the contrary holds true for the fraction of cooperators.

$$\begin{aligned}
\partial_t x_D &= \sum_{i=0}^{G-2} \binom{g}{1+i} x_D^{g-1-i} x_C^{1+i} \frac{(g-1-i)(1+i)}{g(g-1)} \left[ -(-Q\theta(\pi_C - \pi_D)) + Q\theta(\pi_D - \pi_C) \right] \\
&= \sum_{i=0}^{G-2} \binom{g}{1+i} x_D^{g-1-i} x_C^{1+i} \frac{Q(g-1-i)(1+i)}{g(g-1)} \\
&= \sum_{i=0}^{G-2} Q x_D^{g-1-i} x_C^{1+i} \frac{g!(g-1-i)(1+i)}{(g-1-i)!(1+i)!g(g-1)} \\
&= \sum_{i=0}^{G-2} Q x_D^{g-1-i} x_C^{1+i} \frac{(g-2)!}{(g-2-i)!i!} \\
&= Q x_D x_C \sum_{i=0}^{G-2} \binom{g-2}{i} x_D^{g-2-i} x_C^i = Q x_D x_C (x_D + x_C)^{g-2} = Q x_D x_C
\end{aligned} \tag{10}$$

This is precisely the replicator equation which provides a very useful tool for describing the system since its structure does not explicitly depend on  $g$ , even if the evolution itself does, since  $Q$  is a function of  $g$ .

$$\begin{aligned}
\partial_t x_D &= Q x_D x_C \\
\partial_t x_C &= -Q x_D x_C
\end{aligned} \tag{12}$$

The stationary condition yields three possible outcomes,  $x_D = 0, x_C = 0$  and  $Q = 0$ . The first two are the trivial phases of the system, and the third one denotes the critical point, that corresponds to  $r = 1$ . Notice that this condition is reduced to finding the zeros of Eq. (7), and is therefore common for all systems, and independent of their order. This implies that for random uniform hypergraphs cooperators only emerge when  $R > g$ .

If the initial condition is given by a uniform distribution of strategies,  $x_D = x_C = 0.5$ , the time evolution reads

$$\begin{aligned}
x_D(t) &= \frac{1}{1 + e^{Qt}} \\
x_C(t) &= \frac{1}{1 + e^{-Qt}}
\end{aligned} \tag{13}$$

Even if the relaxation time is infinite, we can get the time to arrive the neighbourhood of the asymptotic state by imposing the condition  $x_i = 1/N$  or  $x_i = (N-1)/N$  that yield

$$T = \frac{\ln(N-1)}{|Q|} \quad (14)$$

### C. Replicator Dynamics for HRH

The first thing to notice is that the average payoff difference, is nothing but the sum of the average payoff differences for each of the orders, weighted with the  $p^g$ . The sum goes from  $g^-$ , the minimal value of  $g$  to  $g^+$ , the maximal one.

$$\pi_D - \pi_C = \sum_{g=g^-}^{g^+} p^g (1 - r^g) \quad (15)$$

We first derive the normalization factor  $\Delta$ , from Eq. (9), via the explicit expression for the reduced synergy factor  $r^g = \alpha g^{\beta-1}$ . We consider  $\alpha, \beta \geq 0$ . The extreme point of  $r^g$  at  $\beta = 1$  divides the analysis in two different intervals,  $\beta < 1$  and  $\beta \geq 1$ .

In the first one,  $\beta < 1$ , the maximal payoffs  $\pi^+$  are obtained for the lowest order  $g_-$ , and the minimal payoffs  $\pi^-$  for the highest order  $g_+$ .

$$\pi_D^+ = \alpha g_-^{\beta-1} (g_- - 1), \quad \pi_D^- = 0, \quad \pi_C^+ = \alpha g_-^\beta - 1, \quad \pi_C^- = \alpha g_+^{\beta-1} - 1 \quad (16)$$

Therefore, we get

$$\Delta(\beta < 1) = \begin{cases} \alpha g_-^{\beta-1} (g_- - 1) - \alpha g_+^{\beta-1} + 1 & \text{if } \alpha \leq \frac{2}{g_-^{\beta-1} + g_+^{\beta-1}} \\ \alpha g_-^\beta - 1 & \text{if } \alpha > \frac{2}{g_-^{\beta-1} + g_+^{\beta-1}} \end{cases} \quad (17)$$

In the second interval,  $\beta \geq 1$ , the maximal payoffs are obtained for the maximal orders, and the minimal payoffs for the minimal orders.

$$\pi_D^+ = \alpha g_+^{\beta-1} (g_+ - 1), \quad \pi_D^- = 0, \quad \pi_C^+ = \alpha g_+^\beta - 1, \quad \pi_C^- = \alpha g_-^{\beta-1} - 1 \quad (18)$$

which yields,

$$\Delta(\beta \geq 1) = \begin{cases} \alpha g_+^{\beta-1} (g_+ - 1) - \alpha g_-^{\beta-1} + 1 & \text{if } \alpha \leq \frac{2}{g_-^{\beta-1} + g_+^{\beta-1}} \\ \alpha g_+^\beta - 1 & \text{if } \alpha > \frac{2}{g_-^{\beta-1} + g_+^{\beta-1}} \end{cases} \quad (19)$$

With  $\pi_D - \pi_C$  and  $\Delta$ , we can obtain  $Q$ , as in the uniform case. And in terms of  $Q$  the differential equation for the time evolution is exactly Eq. (12). Therefore, the relaxation time is again given by Eq. (14), and the critical point is again obtained by making  $\pi_D - \pi_C = 0$ , which yields

$$\alpha_c = \frac{1}{\sum_{g=g_-}^{g_+} p^g g^{\beta-1}} \quad (20)$$

#### D. Hypergraphs describing real-world collaborations

*IETF Dataset.* In this last section, we provide an additional practical example of the procedure for extracting the synergy factor from real data, based on the publication records of the Internet Engineering Task Force (IETF). This is a large open international community of network designers, operators, vendors, and researchers concerned with the evolution and the smooth operation of the Internet. Similarly to the APS journals, the system is described by an hypergraph where authors who participated together in a project are part of the same hyperlink. For the IETF dataset, we have 34280 articles. In Fig. 5 we report the histogram of the number of articles with a given number of authors. The normalized version of this histogram is precisely the hyperlink distribution as a function of the order of the hyperlink. Next we retrieve the hyperdegree-order distribution by assuming that the hyperlinks are equally distributed amongst the nodes, meaning that for each order  $g$  the degree can be deduced from the number of links as  $k^g = gL^g/N$ . We assume that the reduced synergy factor is proportional to the hyperdegree distribution. This assumption means that we need an additional parameter to provide the full expression of the reduced synergy factor (and not the normalized one). This parameter can be obtained by introducing the critical point condition  $\sum_{g=g_-}^{g_+} p^g (1 - r(g)) = 0$ . Notice that  $p^g$  is the  $g$ th component of the hyperdegree, and that  $r(g)$  is the synergy factor we are looking for, which can be expressed as  $cp^g$  under the aforementioned assumption. This provides a simple equation to obtain  $c$ ,  $c \sum (p^g)^2 = 1$ , which completes the procedure for extracting  $r(g)$ .

For this particular dataset, for completeness we fit the experimental data with different analytical expressions. We numerically find those parameters that minimize the distance with either  $R(g)$  or  $r(g)$ . To validate the fit, the measure we have selected is the distance between the normalized points of the analytical and the experimental synergy factor, which is bounded to the  $[0, 1]$  interval. Therefore, values close to 0 account for a good estimation of the data, otherwise the opposite is true. To extract the parameters we have performed a search process by limiting the possible values to meaningful regions of the parameter space, and by discretizing this region into a finite set

values. Then, we iterated over all the sets, one for each parameter, and calculated the normalized distance between the analytical expression and the experimental one for each iteration. The best results that we have obtained in Fig. 5 are given by

$$\begin{aligned}
e_1 : r(g) &= \alpha g^\beta e^{-\gamma(g-1)} & (\beta, \gamma) &= (1.382, 0.696) & (d_r, d_R) &= (0.054, 0.090) \\
e_2 : R(g) &= \alpha g^\beta e^{-\gamma(g-1)} & (\beta, \gamma) &= (2.89, 0.865) & (d_r, d_R) &= (0.065, 0.082) \\
e_3 : r(g) &= \alpha g^\beta e^{-\gamma(g-1)^\delta} & (\beta, \gamma, \delta) &= (0.5, 0.12, 1.7) & (d_r, d_R) &= (0.039, 0.079) \\
e_4 : R(g) &= \alpha g^\beta e^{-\gamma(g-1)^\delta} & (\beta, \gamma, \delta) &= (1.51, 0.13, 1.65) & (d_r, d_R) &= (0.041, 0.077)
\end{aligned} \tag{21}$$

Here  $e_i$  is associated to the expressions as reported in the figure,  $\alpha$  is obtained analytically by applying the critical point condition and  $d_r$  and  $d_R$  the distance between the approximation and the points inferred from the data. Notice that the  $(e_1, e_2)$  and  $(e_3, e_4)$  pairs of equations have the same structure, but their parameters have been obtained by minimizing the distance with  $r(g)$  and  $R(g)$ , respectively. As before,  $\beta$  and  $\gamma$  are the benefits and costs fit parameter, that respectively grow as a power law and decrease exponentially.

*APS Dataset.* Here we provide some additional details about the dataset of scientific collaborations from publications in the journals of the American Physical Society described in the main text. In Table I we report the main properties of the hypergraph describing each journal. In addition, we also provide the benefit and cost parameters associated to each journal, as well as the normalized error between the maximum synergy factor extracted directly from the data and from the analytical estimate. In Fig. 6 we show the experimental and approximated reduced synergy factors  $r(g)$  as a function of all hyperlink orders  $g$  contained in the publications dataset. This figure is an extended version of Fig.4(a) in the main dataset.

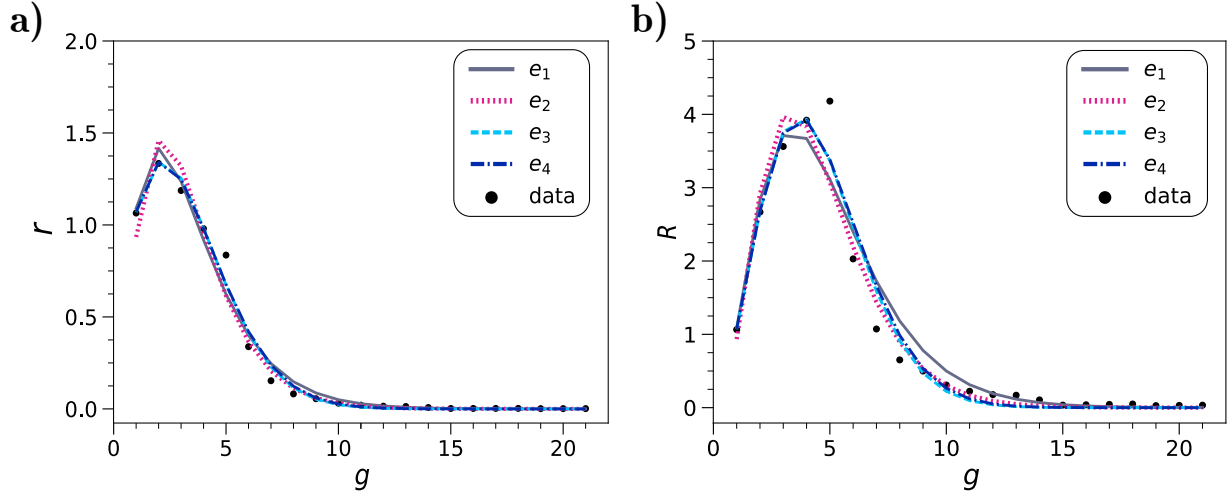


**FIG. 5: Synergy factors of the IETF dataset.** We extract the synergy factor as a function of the group size for a bibliographic dataset in technology that contains the number of publications as a function of the number of authors  $g$ . We infer the distribution in the order of the hyperdegrees from the original dataset by assuming that the hyperlinks are evenly distributed amongst the nodes. We then impose the critical point condition and extract the value of the synergy factor under the hypothesis that  $r(g)$  is proportional to  $p$ . Finally, the synergy factors  $r(g)$  in **(a)** and  $R(g)$  in **(b)** are factorized into two analytical expressions that respectively account for the benefits of large cooperations, and the costs associated to saturation effects.

Journal	$L$	$\langle g \rangle$	$g(\max r)$	$\beta$	$\gamma$	$d_r$
PhysRev	47313	1.95	2	2.936	1.573	0.033
PhysRevA	70502	3.07	3	2.679	0.986	0.067
PhysRevB	171268	3.75	3	1.531	0.49	0.05
PhysRevC	36290	5.98	3	0.02	0.075	0.146
PhysRevD	74715	3.02	2	2.178	0.941	0.206
PhysRevE	50988	2.93	3	3.84	1.41	0.048
PhysRevApplied	327	5.39	5	3.356	0.62	0.09
PhysRevLett	113674	4.57	3	0.848	0.33	0.175
PhysRevSeriesI	1240	1.21	1	2.691	2.831	0.019
PhysRevSTAB	2393	5.52	4	0.566	0.173	0.127
PhysRevSTPER	484	2.42	3	2.75	1.21	0.078
PhysRevX	611	5.28	5	1.85	0.416	0.127
RevModPhys	3153	2.05	2	1.19	0.79	0.112

**TABLE I: APS Dataset.** For each journal we report the total number of hyperlinks  $L$ , the average hyperlink order  $\langle g \rangle$ , the order associated to the maximal synergy factor  $g(\max r)$ , the benefit parameter  $\beta$  and the cost parameter  $\gamma$  (from the analytical approximation of  $r(g)$ ), and the normalized distance between the reduced synergy factor extracted from the data empirically and after the fit, that we indicate as  $d_r$ .

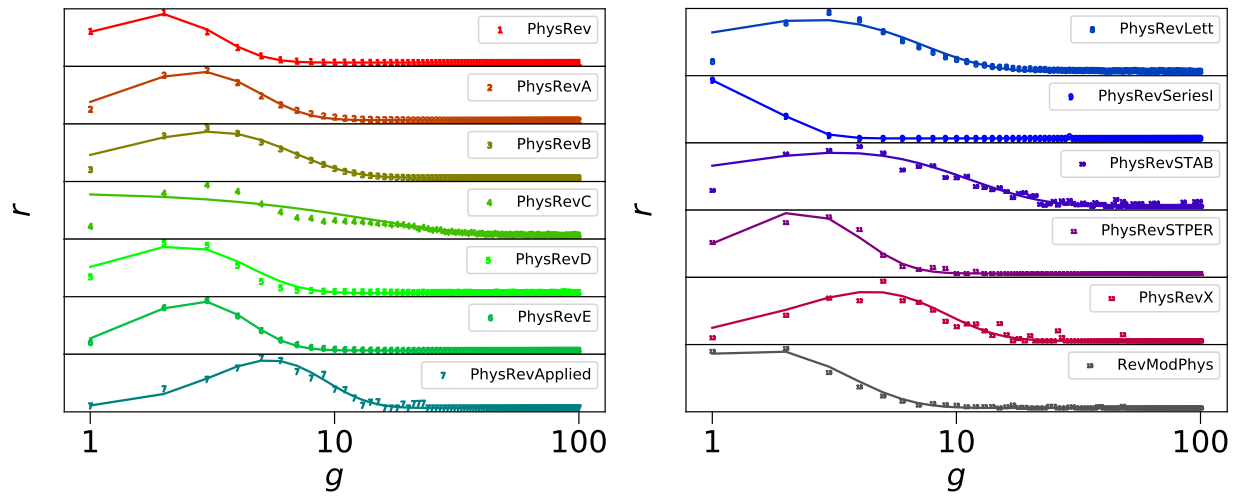


FIG. 6: **Synergy factors of the APS dataset.** Value of the reduced synergy factor  $r(g)$  for all the values of the group size  $g$  available in the dataset. These plots are an extended version of Fig.4 shown in the main manuscript.

## **Acknowledgments**

U.A.-R. acknowledges support from the Spanish Government through Maria de Maeztu excellence accreditation 2018-2022 (Ref. MDM-2017-0714) and from the Basque Government through the Posdoctoral Program (Ref. POS-2017-1-0022). F.B. acknowledges partial support from the ERC Synergy Grant 810115 (DYNASNET). V. L. acknowledges support from the Leverhulme Trust Research Fellowship “CREATE: the network components of creativity and success”. Y. M. acknowledges partial support from the Government of Aragón and FEDER funds, Spain through grant E36-17R to FENOL, by MINECO and FEDER funds (grant FIS2017-87519-P) and from Intesa Sanpaolo Innovation Center. M. P. was supported by the Slovenian Research Agency (Grant Nos. J4-9302, J1-9112, and P1-0403). G. F. A. acknowledges support from Intesa Sanpaolo Innovation Center. We thank M. C. from COSNET Lab for help and assistance with the figures. The funders had no role in study design, data collection, and analysis, decision to publish, or preparation of the manuscript.

## **Author contributions**

U. A.-R, F. B. and V. L. conceived the study with contributions from G. F. A, M. P and Y. M. U. A.-R performed the calculations, U. A.-R, F. B., G. F. A, M. P, Y. M. and V. L. analyzed the data and discussed the results. U. A.-R, F. B., G. F. A, M. P, Y. M. and V. L. wrote the paper.

## **Competing interests**

The authors declare no competing interests.

## **Data availability**

The APS dataset is provided by the APS at their website: <https://journals.aps.org/datasets>.